

OPEN-HOLE TENSION ANALYSIS OF CFRP COMPOSITE USING PROGRESSIVE DAMAGE MODELLING

Mansingh Yadav¹, Nitesh P. Yelve² and Asim Tewari³

¹ IIT Bombay, mansinghyadav8418@gmail.com and <https://mansinghyadav.com/>

² IIT Bombay, nitesh.yelve@iitb.ac.in and <https://www.niteshyelve.com/>

³ IIT Bombay, asim.tewari@iitb.ac.in and <https://www.asimtewari.com/>

Keywords: Drilled-Induced Damages, Digital Image Correlation, Open-Hole Tension, Progressive Damage Modelling.

ABSTRACT

This study aims to develop a 3D progressive damage model (PDM) for analyzing the behavior of fiber-reinforced plastics (FRP) laminates using the open-hole tension test. The proposed PDM is based on a linear damage propagation law and Hashin's 3D failure criterion. To analyze composite laminates, the VUMAT subroutine is incorporated into an Abaqus/explicitTM program. Where, finite element analysis reveals that the strain accumulation around the hole closely resembles the observations made in the experimental study, indicating the presence of stress concentration near the hole. The results demonstrate that the multi-directional [45/-45/0/90]₄ ply sequence experiences strain accumulation and crack propagation primarily in the 45-degree direction. Interlaminar shear and transverse cracking are identified as the primary failure mechanisms in multi-directional ply composite materials.

1 INTRODUCTION

Fiber-reinforced plastic (FRP) composite materials are commonly used in aerospace, automobile, defense, marine, sports, and biomedical applications [1] due to their better mechanical properties, such as high specific stiffness, specific strength, and corrosion resistance. However, FRP composites show complex failure under structural loading conditions due to their non-homogenous and anisotropic behaviour. Therefore, micromechanics of the composite is needed to understand the behaviour of the composites. Progressive damage models (PDM) are popularly used to analyse the failure of FRPs [2]. The PDMs can provide damage initiation and evaluation under complex loading conditions. To foreshow the initiation of damage in laminates made of unidirectional fiber-reinforced plastics (UD-FRP) [3, 21], a number of failure theories exist, among which the Hashin [4], LaRC04 [5], Puck [6], and LaRC05 [7] failure criteria are accepted due to their reasonably precise outcomes.

Several studies have been conducted on the PDM of FRP composites. Early researchers, including Kachanov [8] and Lapczyk and Hurtado [9], developed a model for predicting damage onset and response. A continuum damage model that is based on LaRC04 failure criteria was used by Maimi et al. [10] and Fakoor et al. [11] to explore material softening using different degradation processes. However, instant degradation rules may cause an overestimation of stiffness changes, according to Barbero et al. [12]. The use of PDMs for analysing defects in FRP composites was explored by Nagaraj et al. [13] and Kolor et al. [14], while Yan et al. [15] employed an artificial neural network based PDM to minimize computation costs. Although these PDMs assume an in-plane state of stress and are suitable for thin laminates and in-plane loading, advanced modified models are needed for situations where stress is complex in 3D, such as drilling. To address this, Giasin et al. [16] and Phadnis et al. [17, 18] used finite element modelling with a 3D PDM to simulate drilling. Feito et al. [19] used 3D models to find the delamination during the drilling of CFRP. A drilling-induced delamination model using 3D PDM and Hashin's theory was developed by Isbilir and Ghassemieh [20]. Some studies have also used the cohesive zone method and equivalent strain approach to predict damage evolution under different loading

conditions. However, some models still use instant degradation and mainly predict delamination, which may not be sufficient for complex loading situations.

However, there are many studies that primarily focused on understanding the mechanisms of damage creation during drilling. Not many comprehensive studies have been done to understand the mechanical behaviour of the open-hole tension (OHT) test of FRP composite using 3D PDM. Therefore, this paper numerically explores the effect of the initiation and evolution of the damage in the multi-directional $[45/-45/0/90]_4$ ply sequences. This model analyses the multilayer laminate sequences of CFRP composite and its effect on strain behaviour and load-displacement variation. To begin with, the paper presents an overview of the PDM model, which includes a 3D constitutive relationship between strength and stiffness, as well as a Hashin's 3D failure initiation and linear damage propagation law. Secondly, the paper delves into a discussion of the damage behaviour of a multi-directional $[45/-45/0/90]_4$ ply sequence and validates the findings with experimental results. Lastly, the paper concludes with a summary of the findings in relation to multi-directional $[45/-45/0/90]_4$ ply sequence CFRP composites.

2 MODEL DESCRIPTION

This study aims at developing a 3D PDM to understand the behaviour of CFRP specimens, such as damage initiation and evolution during OHT test. This study is extended further to understand the quasi-static behaviour of open holes in the multi-directional $[45/-45/0/90]_4$ ply sequences composite. The M40J grade CFRP composite material properties, as shown in Table 1, are utilized in the modelling. These layers are connected using cohesive elements. Damage propagation is investigated with a complex 3D state of the stress during OHT test of CFRP composite.

2.1 3D PDM of FRP Composite

This section introduces a method to predict damage in FRP composites. The technique is called mesoscale 3D PDM, as shown in Figure 1, and it relies on continuum damage mechanics. This method assumes that the composite material behaves like a homogenized, linear elastic, and orthotropic material at the mesoscale within a larger laminate. To start the damage process, a technique called 3D Hashin's criterion is used. Then, a linear damage evolution law is added to the process based on how much energy is released. The Abaqus/explicit™ is used to run a model created in the VUMAT subroutine using a Fortran script.

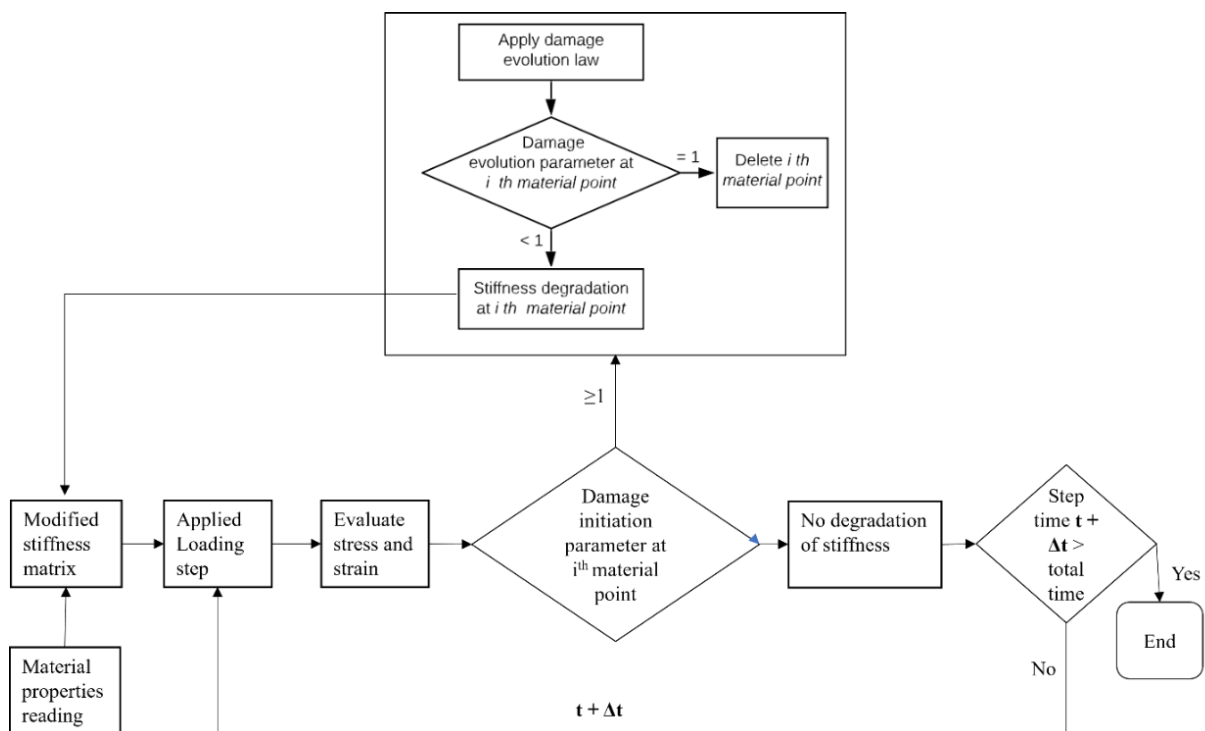


Figure 1: Systematic representation of progressive damage modeling.

2.2 Constitutive Relations

Equation (1) shows the 3D constitutive equations for a UD-FRP lamina, which includes terms for stress, stiffness, and strain. The stiffness terms (C_{ij}) show the stiffness of the lamina before it gets damaged, as defined in Equation (2). These terms can be calculated using Young's modulus and Poisson's ratio, as shown in Equation (3). The constitutive relationship is described in Equation (4), which includes the updated, degraded stiffness terms after damage initiation and throughout the damage evolution process.

$$\begin{Bmatrix} \sigma_{11} \\ \sigma_{22} \\ \sigma_{33} \\ \sigma_{12} \\ \sigma_{23} \\ \sigma_{31} \end{Bmatrix} = \begin{bmatrix} C_{11} & C_{12} & C_{13} & 0 & 0 & 0 \\ C_{12} & C_{22} & C_{23} & 0 & 0 & 0 \\ C_{13} & C_{23} & C_{33} & 0 & 0 & 0 \\ 0 & 0 & 0 & 2G_{12} & 0 & 0 \\ 0 & 0 & 0 & 0 & 2G_{23} & 0 \\ 0 & 0 & 0 & 0 & 0 & 2G_{31} \end{bmatrix} \begin{Bmatrix} \varepsilon_{11} \\ \varepsilon_{22} \\ \varepsilon_{33} \\ \varepsilon_{12} \\ \varepsilon_{23} \\ \varepsilon_{31} \end{Bmatrix}. \quad (1)$$

$$C_{11} = \frac{(1 - v_{23}v_{32})}{E_2E_3\Delta}; \quad C_{12} = \frac{(v_{21} + v_{23}v_{31})}{E_2E_3\Delta}; \quad C_{13} = \frac{(v_{31} + v_{21}v_{32})}{E_2E_3\Delta}; \quad (2)$$

$$C_{23} = \frac{(v_{32} + v_{12}v_{31})}{E_1E_3\Delta}; \quad C_{22} = \frac{(1 - v_{13}v_{31})}{E_1E_3\Delta}; \quad C_{33} = \frac{(1 - v_{12}v_{21})_{SS}}{E_1E_2\Delta}.$$

$$\Delta = \frac{(1 - v_{12}v_{21} - v_{23}v_{32} - v_{13}v_{31} - 2v_{21}v_{32}v_{13})}{E_1E_2E_3}. \quad (3)$$

$$\begin{Bmatrix} \sigma_{11} \\ \sigma_{22} \\ \sigma_{33} \\ \sigma_{12} \\ \sigma_{23} \\ \sigma_{31} \end{Bmatrix} = \begin{bmatrix} C_{11}^d & C_{12}^d & C_{13}^d & 0 & 0 & 0 \\ C_{12}^d & C_{22}^d & C_{23}^d & 0 & 0 & 0 \\ C_{13}^d & C_{23}^d & C_{33}^d & 0 & 0 & 0 \\ 0 & 0 & 0 & 2G_{12}^d & 0 & 0 \\ 0 & 0 & 0 & 0 & 2G_{23}^d & 0 \\ 0 & 0 & 0 & 0 & 0 & 2G_{31}^d \end{bmatrix} \begin{Bmatrix} \varepsilon_{11} \\ \varepsilon_{22} \\ \varepsilon_{33} \\ \varepsilon_{12} \\ \varepsilon_{23} \\ \varepsilon_{31} \end{Bmatrix}, \quad (4)$$

where, $C_{11}^d = (1 - d_f)C_{11}$; $C_{12}^d = (1 - d_f)(1 - d_m)C_{12}$; $C_{13}^d = (1 - d_f)(1 - d_m)C_{13}$,
 $C_{22}^d = (1 - d_m)C_{22}$; $C_{33}^d = (1 - d_m)C_{33}$; $C_{23}^d = (1 - d_f)(1 - d_m)C_{23}$, and
 $G_{12}^d = (1 - d_s)G_{12}$; $G_{23}^d = (1 - d_s)G_{23}$; $G_{31}^d = (1 - d_s)G_{31}$. (5)

The stiffness matrix in Equation (5) shows how the stiffness of the ply gets weaker after damage occurs and it can be calculated using the damage variables from equation (6). The damage variables d_f , d_m , and d_s represent the degree of damage for the fibers, matrix, and shear, respectively.

$$d_f = 1 - (1 - d_{ft})(1 - d_{fc}),$$

$$d_m = 1 - (1 - d_{mt})(1 - d_{mc}), \text{ and} \quad (6)$$

$$d_s = 1 - (1 - d_{ft})(1 - d_{fc})(1 - d_{mt})(1 - d_{mc}).$$

The symbols d_{mt} and d_{mc} represent the matrix's damage modes in tension and compression, respectively. The symbols d_{ft} , and d_{fc} are used to represent the damage modes of the fiber in tension and compression, respectively.

E_1 (GPa)	E_2 (GPa)	G_{12} (GPa)	V_{12}	X_T (MPa)	X_C (MPa)	Y_T (MPa)
232	9.8	4.5	0.3	2400	1050	24
Y_C (MPa)	S_L (MPa)	S_T (MPa)	G_{ft} (N/mm)	G_{fc} (N/mm)	G_{mt} (N/mm)	G_{mc} (N/mm)
145	59	59	70	70	0.25	0.25

Table 1. Elastic properties, strength properties, and damage parameters of M40J CFRP composite [22, 23].

2.3 Damage initiation

3D Hashin's theory [4] predicts the initiation of damage in UD FRP laminate. This theory can identify various damage modes and is helpful for gradual damage analysis. The theory works by using effective stresses (represented by $\tilde{\sigma}_{ij}$) that act on a particular point and initiate one of the 4 damage mechanisms: matrix tension, fiber tension, matrix compression, and fiber compression. The effective stresses are created by combining the damage tensor (M) calculated using Equation (7) and the nominal stresses.

$$\tilde{\sigma} = M\sigma; M = \text{diag} \left(\frac{1}{1-d_f}, \frac{1}{1-d_m}, \frac{1}{1-d_m}, \frac{1}{1-d_s}, \frac{1}{1-d_s}, \frac{1}{1-d_s} \right) \quad (7)$$

In Equations (8 - 11), 3D Hashin's onset of damage demonstrated. The variables d_s , d_m , and d_f refer to the extent of damage caused by shear, matrix, and fiber damage, respectively from Equation (6).

Tensile fiber mode: $\tilde{\sigma}_{11} \geq 0$

$$F_{ft} = \left(\frac{\tilde{\sigma}_{11}}{X_{1t}} \right)^2 + \left(\frac{\tilde{\sigma}_{12}}{S_{12}} \right)^2 + \left(\frac{\tilde{\sigma}_{13}}{S_{13}} \right)^2. \quad (8)$$

Compressive fiber mode: $\tilde{\sigma}_{11} < 0$

$$F_{fc} = \frac{|\tilde{\sigma}_{11}|}{X_{1c}}. \quad (9)$$

Tensile matrix mode: $\tilde{\sigma}_{22} + \tilde{\sigma}_{33} \geq 0$

$$F_{mt} = \left(\frac{\tilde{\sigma}_{22} + \tilde{\sigma}_{33}}{X_{2t}} \right)^2 + \frac{\tilde{\sigma}_{12}^2}{S_{12}^2} + \frac{\tilde{\sigma}_{13}^2}{S_{13}^2} + \frac{\tilde{\sigma}_{23}^2 - \tilde{\sigma}_{22}\tilde{\sigma}_{33}}{S_{23}^2}. \quad (10)$$

Compressive matrix mode: $\tilde{\sigma}_{22} + \tilde{\sigma}_{33} < 0$

$$F_{mc} = \left(\frac{\tilde{\sigma}_{22} + \tilde{\sigma}_{33}}{2S_{23}} \right)^2 + \left(\frac{\tilde{\sigma}_{22} + \tilde{\sigma}_{33}}{X_{2c}} \right) \left[\frac{X_{2c}^2}{2S_{23}^2} - 1 \right] + \frac{\tilde{\sigma}_{12}^2}{S_{12}^2} + \frac{\tilde{\sigma}_{13}^2}{S_{13}^2} + \frac{\tilde{\sigma}_{23}^2 - \tilde{\sigma}_{22}\tilde{\sigma}_{33}}{S_{23}^2}. \quad (11)$$

F_{ft} , F_{fc} , F_{mt} , and F_{mc} represent the beginning of damage in respective modes. They range from 0 to 1, with one being the critical value for damage initiation. Once one of these variables reaches 1, damage occurs in that mode.

2.4 Damage propagation

Once damage initiates in the UD-FRP lamina, its behavior changes. At first, it is linearly elastic, following Equation (1). But as the loading continues, the stiffness of the lamina deteriorates, which is reflected in the updated stiffness matrix and incorporated into Equation (5). Equation (6) controls the degradation through global damage variables, which are calculated by assigning a local damage variable to each of the 4 damage modes and using Equation (12) to predict them. The local damage variable takes a value between 0 (undamaged) and 1 (fully damaged).

$$d_i = \frac{\varepsilon_{eq}^{f,i}(\varepsilon_{eq}^i - \varepsilon_{eq}^{o,i})}{\varepsilon_{eq}^i(\varepsilon_{eq}^{f,i} - \varepsilon_{eq}^{o,i})} \quad (i = ft, fc, mt, mc) \quad (12)$$

Equivalent strains at the onset of damage and fracture represented by $\varepsilon_{eq}^{o,i}$ and $\varepsilon_{eq}^{f,i}$ in a 3D state of strain are represented by Equations (13) to (16).

- Fiber tension:

$$\varepsilon_{eq}^{ft} = \sqrt{\langle \varepsilon_{11} \rangle^2 + \varepsilon_{12}^2 + \varepsilon_{13}^2}; \quad \varepsilon_{eq}^{o,ft} = \frac{X_{1t}}{E_1}; \quad \varepsilon_{eq}^{f,ft} = \frac{2G_c^{ft}}{X_{1t}L_c}. \quad (13)$$

- Fiber compression:

$$\varepsilon_{eq}^{fc} = \langle -\varepsilon_{11} \rangle; \quad \varepsilon_{eq}^{o,fc} = \frac{X_{1c}}{E_1}; \quad \varepsilon_{eq}^{f,fc} = \frac{2G_c^{fc}}{X_{1c}L_c}. \quad (14)$$

- Matrix tension:

$$\varepsilon_{eq}^{mt} = \sqrt{\langle \varepsilon_{22} \rangle^2 + \langle \varepsilon_{33} \rangle^2 + \varepsilon_{12}^2 + \varepsilon_{13}^2}; \quad \varepsilon_{eq}^{o,mt} = \frac{X_{2t}}{E_2}; \quad \varepsilon_{eq}^{f,mt} = \frac{2G_c^{mt}}{X_{2t}L_c}. \quad (15)$$

- Matrix compression:

$$\varepsilon_{eq}^{mc} = \sqrt{\langle -\varepsilon_{22} \rangle^2 + \langle -\varepsilon_{33} \rangle^2 + \varepsilon_{12}^2 + \varepsilon_{13}^2}; \quad \varepsilon_{eq}^{o,mc} = \frac{X_{2c}}{E_2}; \quad (16)$$

$$\varepsilon_{eq}^{f,mc} = \frac{2G_c^{mc}}{X_{2c}L_c}.$$

2.5 FE model

To create a more detailed mesh around the hole and its surroundings, mesh partitioning is used, as shown in Figure 2(a). This involves cutting through a datum plane using a three-point method to generate a finer mesh. A coarse mesh is used globally to save time. Mesh control uses the Hex element shape with sweep technique, and the explicit element type is selected with 3D stress of linear geometric order (C3D8R). To analyze the behavior of the laminate with open-hole, a displacement-controlled tension load is applied, as shown in Figure 2(b). The material properties listed in Table 1 are used for the material model.

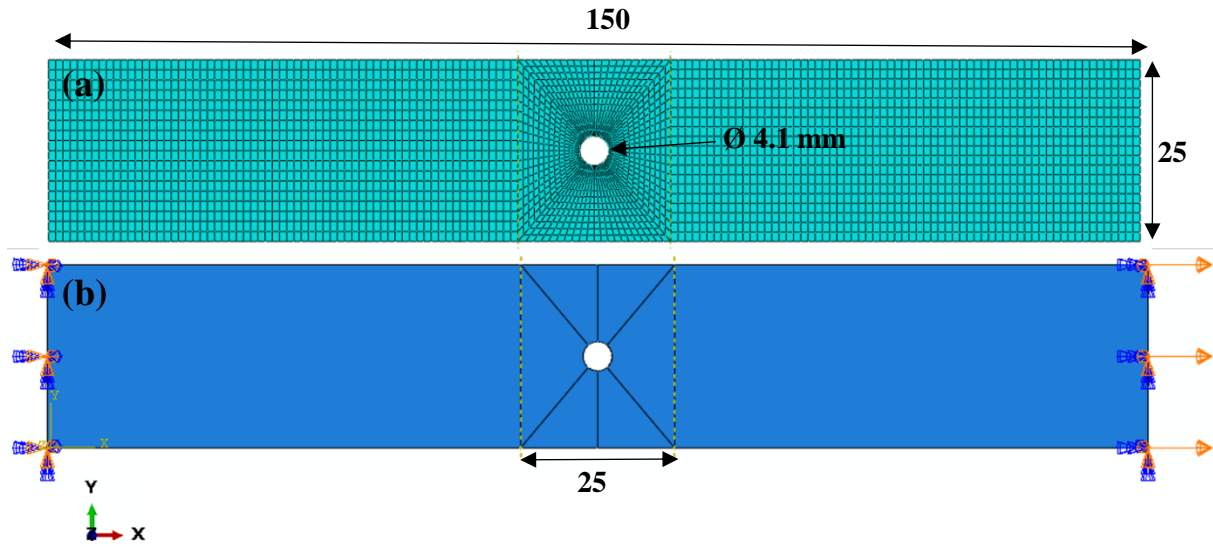


Figure 2: (a) Local and global meshing of the sample (b) Displacement-control loading of the sample.

3 RESULTS AND DISCUSSION

In this section, the performance of the PDM during the quasi-static loading is determined. Damage initiates around the hole, degrading the strength and stiffness with its propagation. There is strain fringing around the hole, which varies with the load application. The stress concentration around the hole depends on parameters such as fiber orientation, drilling parameters, and materials. The UD-FRP lamina behaves under uniaxial loading, as shown in Figure 3. It starts with a linear elastic response (AB) until it reaches the point of damage initiation, B ($d_i=0$). After that point, its stiffness gradually decreases (BC) due to damage evolution until it reaches the fracture point, C ($d_i=1$). For instance, the stiffness at point B is greater than at any point on the damage propagation line BC . In Figure 4, the results of a finite element analysis are presented. In 4(a), the initiation of damage in the composite due to quasi-static tension loading at the open hole is shown. This damage initiation and subsequent propagation cause a degradation in the stiffness and strength of the composite. Similarly, Figure 4(b) shows the propagation of damage. Figures 4(c) and 4(d) depict the initiation and propagation of the crack in the matrix phase, which also affects the mechanical properties of the composite.

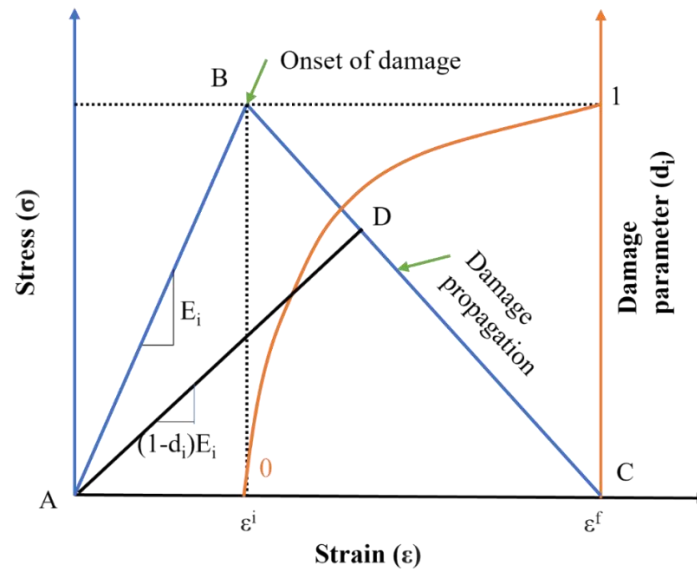


Figure 3: Schematic of stress and damage parameters response with changes in strain.

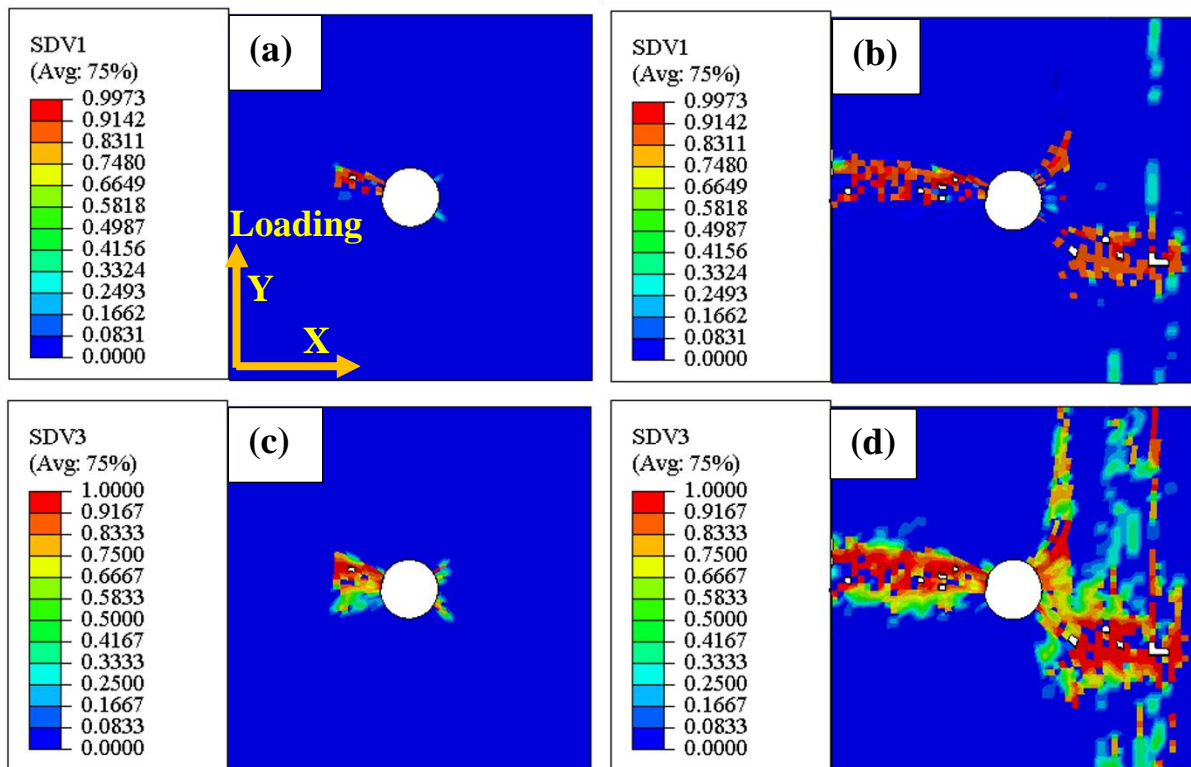


Figure 4: FE analysis results of open-hole quasi-static tension test for multi-directional $[45/-45/0/90]_4$ ply sequence (a) Fiber damage initiation (b) Fiber damage evolution (c) Matrix damage initiation (d) Matrix damage evolution.

During the quasi-static tension test of a CFRP composite with DIC, strain distribution analysis is carried out to observe its behavior under loading. The following observations are made, as shown in Figure 5. A localized strain concentration can be seen around the open hole in the specimen, indicating stress built-up (Figure 5(a)). The strain distribution can be used to determine the location and size of the stress concentration. Strain discontinuities or concentration at localize zone shows the damage initiation

(Figure 5(b)) wherein further application of load leads to the damage propagation, and finally, fracture occurs as shown in Figure 5(c). Strain distribution can be used to locate any anisotropy behavior in the material, which is common in CFRP composites due to their highly anisotropic mechanical properties. Any regions where strain values differ significantly may indicate localized defects or material damage.

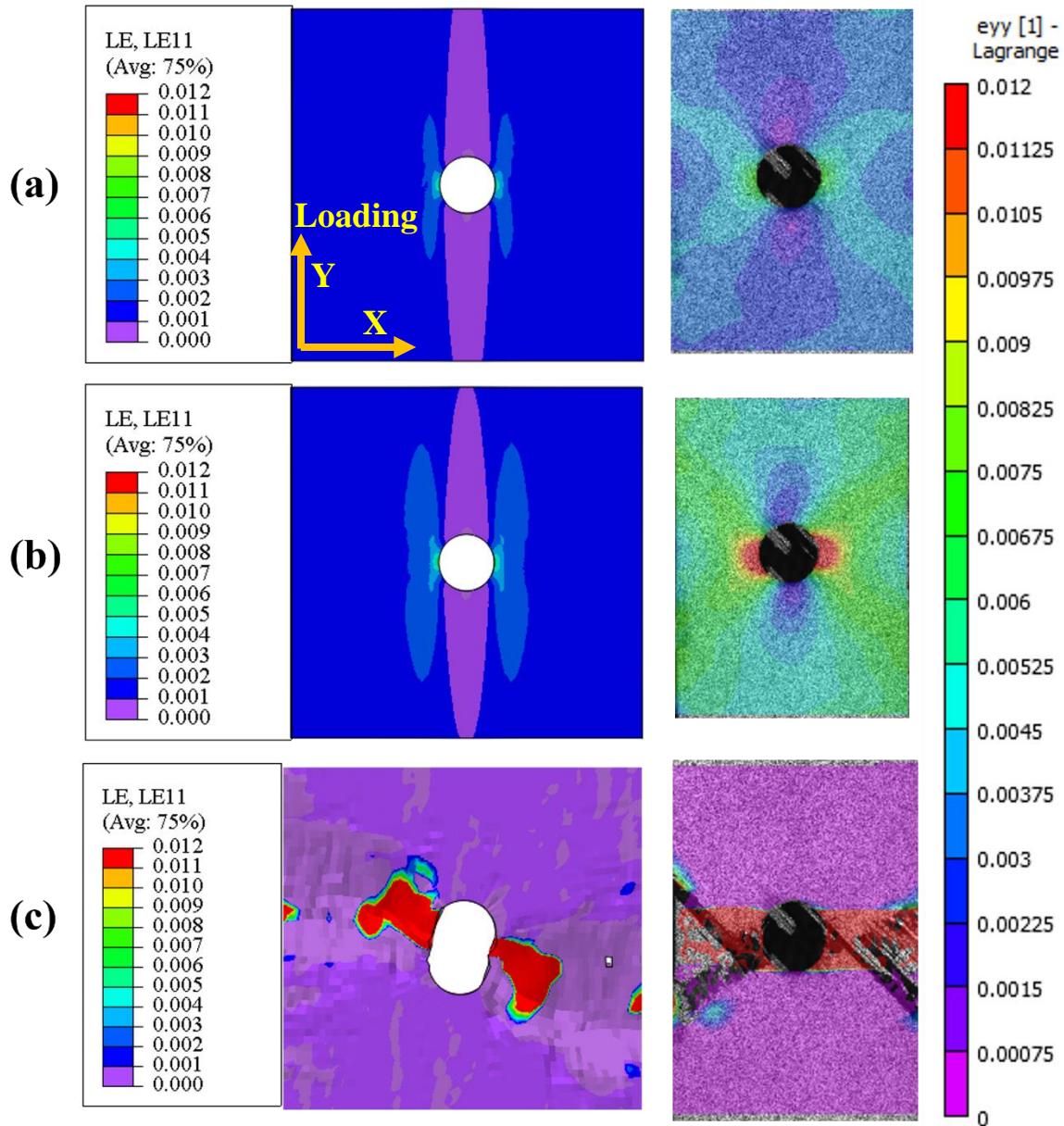


Figure 5: Strain mapping of multi-directional ply at different phases (a) localized strain concentration (b) damage initiation (c) fracture condition.

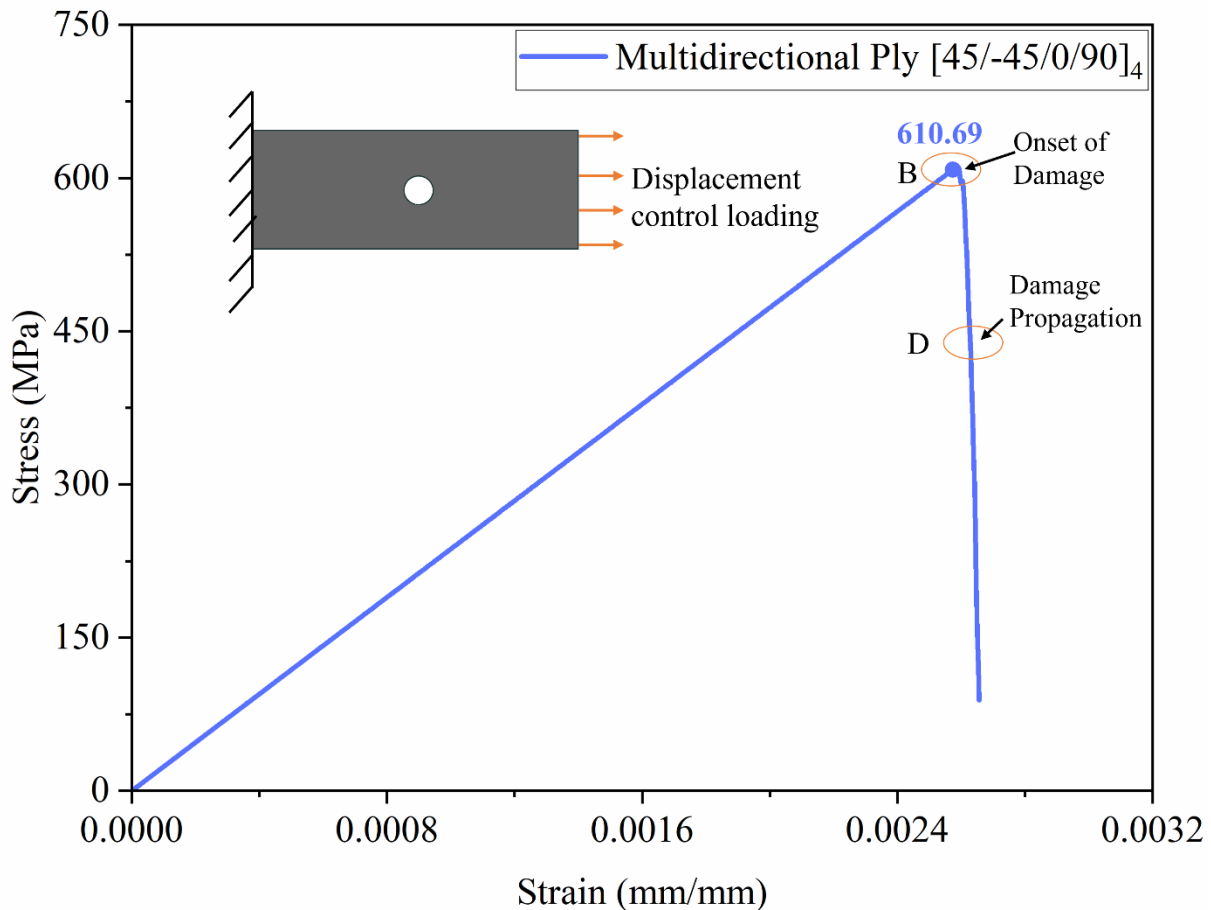


Figure 6: *FE* results for stress variation with strain during uniaxial tension.

The stress vs strain curve obtained from the test provides information about the stiffness, yield strength of the material, and failure behavior. In Figure 6, the elastic region of the curve represents elastic response of the composite, while the yielding region corresponds to plastic deformation and necking near the drilled hole. The failure point indicates the strength and susceptibility to failure in specific regions in the composite material. This information can be used to optimize the design and performance of composite structures for high-stress environments.

4 CONCLUSIONS

The experimental study validated the results obtained from the FE analysis, leading to the following conclusions. Firstly, strain accumulation around the hole is similar in the FE and experiment analyses. This is due to stress built-up near the hole. Secondly, in the multi-directional [45/-45/0/90]₄ ply sequence, strain accumulation and crack propagation occur in the 45-degree direction. Finally, interlaminar shear and transverse cracking are the primary causes of failure for multi-directional [45/-45/0/90]₄ ply composite materials. The results from the experiment can be further used to determine the tensile strength, stiffness, and strain of the composite material. Through the proper understanding of stress concentration spreading around an open hole in a particular sequence of CFRP composite, it is possible to prevent damage initiation and evolution through the proper selection of geometric and process parameters.

ACKNOWLEDGEMENTS

This research was partially supported by The Prime Minister's Research Fellowship (PMRF) and Advanced Fiber Reinforced Polymer Composite Development Center (AFRPCDC) under the Technology Mission on Technical Textile (TMTT) at IIT-Bombay (P16TEXT001).

REFERENCES

- [1] Jones, Robert M. Mechanics of composite materials. CRC press, 2018
- [2] Oya, N. and Hamada, H., 1997. Mechanical properties and failure mechanisms of carbon fibre reinforced thermoplastic laminates. *Composites Part A: Applied Science and Manufacturing*, 28(9-10), pp.823-832 (doi: [10.1016/S1359-835X\(97\)00035-3](https://doi.org/10.1016/S1359-835X(97)00035-3)).
- [3] Li, S. and Sitnikova, E., 2018. A critical review on the rationality of popular failure criteria for composites. *Composites Communications*, 8, pp.7-13 (doi: [10.1016/j.coco.2018.02.002](https://doi.org/10.1016/j.coco.2018.02.002)).
- [4] Hashin, Z., 1980. Fatigue Failure Criteria for Unidirectional Fiber Composites. Pennsylvania Univ Philadelphia Dept of Materials Science and Engineering (doi: [10.1115/1.3153664](https://doi.org/10.1115/1.3153664)).
- [5] Pinho, S.T., Dávila, C.G., Camanho, P.P., Iannucci, L. and Robinson, P., 2005. Failure models and criteria for FRP under in-plane or three-dimensional stress states including shear non-linearity (No. NASA/TM-2005-213530).
- [6] Puck, A. and Schürmann, H., 2002. Failure analysis of FRP laminates by means of physically based phenomenological models. *Composites science and technology*, 62(12-13), pp.1633-1662 (doi: [10.1016/S0266-3538\(01\)00208-1](https://doi.org/10.1016/S0266-3538(01)00208-1)).
- [7] Pinho, S.T., Darvizeh, R., Robinson, P., Schuecker, C. and Camanho, P.P., 2012. Material and structural response of polymer-matrix fibre-reinforced composites. *Journal of Composite Materials*, 46(19-20), pp.2313-2341 (doi: [10.1177/0021998312454478](https://doi.org/10.1177/0021998312454478)).
- [8] Kachanov, M., 1994. On the concept of damage in creep and in the brittle-elastic range. *international Journal of DAMAGE MECHANICS*, 3(4), pp.329-337 (doi: [10.1177/105678959400300402](https://doi.org/10.1177/105678959400300402)).
- [9] Lapczyk, I. and Hurtado, J.A., 2007. Progressive damage modeling in fiber-reinforced materials. *Composites Part A: Applied Science and Manufacturing*, 38(11), pp.2333-2341 (doi: [10.1016/j.compositesa.2007.01.017](https://doi.org/10.1016/j.compositesa.2007.01.017)).
- [10] Maimí, P., Camanho, P.P., Mayugo, J.A. and Dávila, C.G., 2007. A continuum damage model for composite laminates: Part II—Computational implementation and validation. *Mechanics of materials*, 39(10), pp.909-919 (doi: [10.1016/j.mechmat.2007.03.006](https://doi.org/10.1016/j.mechmat.2007.03.006)).
- [11] Fakoor, M. and Ghoreishi, S.M.N., 2018. Experimental and numerical investigation of progressive damage in composite laminates based on continuum damage mechanics. *Polymer Testing*, 70, pp.533-543 (doi: [10.1016/j.polymertesting.2018.08.013](https://doi.org/10.1016/j.polymertesting.2018.08.013)).
- [12] Barbero, E.J., Cosso, F.A., Roman, R. and Weadon, T.L., 2013. Determination of material parameters for Abaqus progressive damage analysis of E-glass epoxy laminates. *Composites Part B: Engineering*, 46, pp.211-220 (doi: [10.1016/j.compositesb.2012.09.069](https://doi.org/10.1016/j.compositesb.2012.09.069)).
- [13] Nagaraj, M.H., Reiner, J., Vaziri, R., Carrera, E. and Petrolo, M., 2020. Progressive damage analysis of composite structures using higher-order layer-wise elements. *Composites Part B: Engineering*, 190, p.107921 (doi: [10.1016/j.compositesb.2020.107921](https://doi.org/10.1016/j.compositesb.2020.107921)).
- [14] Kolor, S.S.R., Khosravani, M.R., Hamzah, R.I.R. and Tamin, M.N., 2018. FE model-based construction and progressive damage processes of FRP composite laminates with different manufacturing processes. *International Journal of Mechanical Sciences*, 141, pp.223-235 (doi: [10.1016/j.ijmecsci.2018.03.028](https://doi.org/10.1016/j.ijmecsci.2018.03.028)).
- [15] Yan, S., Zou, X., Ilkhani, M. and Jones, A., 2020. An efficient multiscale surrogate modelling framework for composite materials considering progressive damage based on artificial neural networks. *Composites Part B: Engineering*, 194, p.108014 (doi: [10.1016/j.compositesb.2020.108014](https://doi.org/10.1016/j.compositesb.2020.108014)).

- [16] Giasin, K., Ayvar-Soberanis, S., French, T. and Phadnis, V., 2017. 3D finite element modelling of cutting forces in drilling fibre metal laminates and experimental hole quality analysis. *Applied Composite Materials*, 24, pp.113-137 (doi: [10.1007/s10443-016-9517-0](https://doi.org/10.1007/s10443-016-9517-0)).
- [17] Phadnis, V.A., Makhdam, F., Roy, A. and Silberschmidt, V.V., 2012. Drilling-induced damage in CFRP laminates: Experimental and numerical analysis. In *Solid State Phenomena* (Vol. 188, pp. 150-157). Trans Tech Publications Ltd (doi: [10.4028/www.scientific.net/SSP.188.150](https://doi.org/10.4028/www.scientific.net/SSP.188.150)).
- [18] Phadnis, V.A., Makhdam, F., Roy, A. and Silberschmidt, V.V., 2013. Drilling in carbon/epoxy composites: Experimental investigations and finite element implementation. *Composites Part A: Applied Science and Manufacturing*, 47, pp.41-51 (doi: [10.1016/j.compositesa.2012.11.020](https://doi.org/10.1016/j.compositesa.2012.11.020)).
- [19] Feito, N., López-Puente, J., Santiuste, C. and Miguélez, M.H., 2014. Numerical prediction of delamination in CFRP drilling. *Composite Structures*, 108, pp.677-683 (doi: [10.1016/j.compstruct.2013.10.014](https://doi.org/10.1016/j.compstruct.2013.10.014)).
- [20] Isbilir, O. and Ghassemieh, E., 2013. Numerical investigation of the effects of drill geometry on drilling induced delamination of carbon fiber reinforced composites. *Composite Structures*, 105, pp.126-133 (doi: [10.1016/j.compstruct.2013.04.026](https://doi.org/10.1016/j.compstruct.2013.04.026)).
- [21] Divse, V., Marla, D., & Joshi, S. S. (2022). 3D progressive damage modeling of fiber reinforced plastics laminates including drilling-induced damage. *Composites Part A: Applied Science and Manufacturing*, 163, 107230.
- [22] Wang, X., Li, W., Guan, Z., Li, Z., Wang, Y., Zhang, M., ... & Du, S. (2019). Clustering effect on mechanical properties and failure mechanism of open hole high modulus carbon fiber reinforced composite laminates under compression. *Composite Structures*, 229, 111377.
- [23] Shin, D. K., Kim, H. C., & Lee, J. J. (2014). Numerical analysis of the damage behavior of an aluminum/CFRP hybrid beam under three point bending. *Composites Part B: Engineering*, 56, 397-407.